Journal: WES
Title: Performance study of the QuLAF pre-design model for a 10MW floating wind turbine
Author(s): Freddy J. Madsen et al.
MS No.: wes-2019-20
MS Type: Research articles

Referee 1 - Anonymous

The authors thank the referee for the suggestions, comments and insights, which has led to improvement of the paper. Please find below the referee's comments (RC), the corresponding author's comments (AC) and the changes in the manuscript. PXLY refers to page X and line Y in the ***revised*** manuscript.

RC: The paper clearly shows that QuLAF can either under-predict or over-predict the results from FAST, and can sometimes match them perfectly through a favorable combination of discrepancies. For example, the authors show that for DLC1.6, a perfect match between the two models in tower base bending moments is obtained. However, this perfect march results from opposite discrepancies which cancel one another. In such a case, the reliability of the approach can be questionable as a good result is obtained for "bad reasons". Although the tool is of course intended for use in a pre-design phase, it would be useful if the authors could elaborate more on the reliability/repeatability of such results for different conditions and design types.

AC: Agree. The shortcomings of the QuLAF model observed for wave-dominated or wind-dominated situations are sometimes cancelling each other when combined wind and waves are applied (as in DLC1.6) for the present floater. We have updated the text to make it clearer and to emphasize this cancellation effect (see P12L10). The authors also point out that this "lucky" cancellation effect is no specific to this model only, but it can also show when e.g. comparing state-of-the-art numerical results to experimental measurements.

RC: Additionally, the QuLAF approach is restricted to 2D analyses with aligned wind and waves. It also models different physics than FAST (e.g. the mooring system in FAST introduces different sources of damping). More insights could be given on how these assumptions are likely to affect the accuracy and reliability of the results for different designs.

AC: The model is meant to complement existing state-of-the-art tools, giving a preliminary quick overview of the response and loads for a wide range of environmental conditions. After this preliminary screening, the time-domain model should be used to analyze in more detail specific load cases - e.g. cases with extreme loads or transient events (see P3L22-24 and P32L16-22). We have included a sentence on mooring in P4L20.

RC: P. 4 L. 27: An estimation of how much faster QuLAF is compared to FAST could be valuable

AC: We agree that this information would be valuable for the paper. We have added a comment on P4L4 regarding the computational times.

Please note that other minor changes have been introduced in the text to improve readability and fix a few typos.

Journal: WES
Title: Performance study of the QuLAF pre-design model for a 10MW floating wind turbine
Author(s): Freddy J. Madsen et al.
MS No.: wes-2019-20
MS Type: Research articles

Referee 2 – Maurizio Collu

The authors thank the referee for the suggestions, comments and insights, which has led to improvement of the paper. Please find below the referee's comments (RC), the corresponding author's comments (AC) and the changes in the manuscript. PXLY refers to page X and line Y in the ***revised*** manuscript.

RC: The only main comment I have is the following: precise quantitative differences between the results obtained in FAST and QuLAF are presented, but they are qualitatively classified as “good”, “acceptable”, and so on. It is not clear to me what is the criterion utilised to judge the goodness of the results, i.e. what would be the “unsuitable/acceptable/good/very good” thresholds (i.e. 30%/25%/10%/5% ? Different for different parameters?), based on state-of-the-art industry experience. I can appreciate that it is always difficult to have some precise numbers, but since this work has been carried out as part of the EU project Lifes50+ I wonder if the authors could add a discussion regarding this aspect, taking advantage of the close collaboration with some of the main FOWT support structure designers during the project.

AC: AC: We agree with the referee that it was not very clear. Effort has now been put into streamlining the classifications of the results – utilizing: 0-5% (very good), 5-10% (good), 10-15% (fairly good) and 15-20% disagree. We have updated the results discussions in section 5. Our general comprehension is that in the pre-design phase you can accept lower accuracy just that the trends are rights.

RC: Pag.6, line 19: “Six different wind and wave seeds were simulated for each environmental condition” and, later “a simulation time of 5400s with the same length of turbulent wind field was used for all the load cases including 1800s run-in-time to remove any transient response in the time-domain model”. Does it mean that transient (1800) + 6 x 10 minutes simulations (each one with a different wind and wave seeds) have been adopted?

AC: We did not carry out any 10 min simulations. Each simulation of 90min (30min transient) is done for a specific peak period, wind/wave seed and mean wind speed, i.e. (7 wind speeds x 3 peak periods x 6 seeds) x 5400s. We have extended Table 3 on page 7 to include number of simulations per load.

RC: Pag.14, line 11: “The deviation levels in Table 8 are of the same magnitude and the reason for this is that only maximum values have been considered in the table. This might not be representative for this transient load case, where also the negative values have high influence, as can be seen in the left column of Figure6.” Would it be possible to add a table relative to the max (in module) negative values, and discuss these as done for the max (in module) positive values?

AC: We agree and thank the referee for the comment. We have extended Table 8, page 15, the discussion and included Figure 7, page 16 with time series to clarify.

RC: Pag.2, line 7: “especially if they are carried out with time-domain numerical tools simulating at real-time CPU speed” Please clarify what it is meant by “at real-time CPU speed”, indicating the simulated-to-simulation time ratio.

AC: Yes, by “real-time CPU” we mean a simulated-to-simulation time ratio of 1. We have updated the text, see P2L8.

RC: Pag.2, line 10: “when the concept design is more converged”, please re-phrase, not very clear.

AC: We changed “converged” to “refined” (P2L11).

Journal: WES
Title: Performance study of the QuLAF pre-design model for a 10MW floating wind turbine
Author(s): Freddy J. Madsen et al.
MS No.: wes-2019-20
MS Type: Research articles

RC: Pag.10, caption of Table 5, please re-phrase expanding it (at the moment a bit difficult to understand).

AC: We agree. We changed all the captions of the result-tables to make it more clear (Table 5-9).

RC: Pag.15: "The simulations consists of 18 realizations (i.e. six seeds)" How long each simulation? Would it be possible to summarise the info below, adding them as additional columns on the right in Table 5? - Length of simulation - Timestep of integration - Number of seeds (and how many minutes for each seed).

AC: We thank the referee for the suggestion. We have adapted the idea into Table 5.

RC: Fig.9 The names of the load cases seem to be the names of the files used – i.e. not very clear. Furthermore, some of them are cut, and in general very small to be read. It is more important to highlight the fact that FAST and QuLAF agree or disagree on the load case ranking, than the specific name of the load case.

AC: The figure was indeed not very clear. We have changed the layout and labelling of the bars on Figure 10, page 20 so it is easier to read. As the reviewer writes, the reason for having this figure is to highlight the agreement or disagreement on the load case ranking.

Please note that other minor changes have been introduced in the text to improve readability and fix a few typos.

Journal: WES
Title: Performance study of the QuLAF pre-design model for a 10MW floating wind turbine
Author(s): Freddy J. Madsen et al.
MS No.: wes-2019-20
MS Type: Research articles

Referee 3 – Tor A. Nygaard

The authors thank the referee (and the additional contributors) for the suggestions, comments and insights, which has led to improvement of the paper. Please find below the referee's comments (RC), the corresponding author's comments (AC) and the changes in the manuscript. PXLY refers to page X and line Y in the ***revised*** manuscript.

RC: Although QuLAF is well described in the references, many of the readers working on floating wind turbines have most experience with time domain models, and I think the article would benefit from some clarifications.

AC: We agree that a more extended description of the model would be helpful. We chose the present quite short description to save on paper length and to avoid overlap with the original QuLAF paper which is also published in Wind Energy Science. The model is extensively described in the companion paper by Pegalajar-Jurado et al. (2018), where the frequency-domain solution is introduced and compared to the time-domain solution.

RC: In the left plots of figure 2, we have several results for each wind speed. The way I read the paper, for each wind speed, three sets of Hs and Tp are generated from the joint probability distribution. Each of these three realizations are computed with six different wind and wave seeds (also realizations). If indeed the use of several wind and wave seeds for one particular combination of Vm, Hs and Tp are used for the frequency domain model, please explain why this is done. Many frequency domain models work with distributions as input and output, directly giving the results for an infinite number of realizations. Here, however, does the input to QuLAF contains phase information for the particular realization at hand? Can the QuLAF results then be transformed back to the time domain, to be directly compared with the time domain FAST results, and post-processed with the same methods, such as rainflow counting?

AC: Yes, QuLAF contains phase information, since time-series of precomputed aerodynamic loads and free-surface elevation are input to the model. As a consequence, time-series of the results are available for comparison to time-domain models and for further analysis (note that fatigue damage-equivalent loads at the tower base are one of the metrics in this paper and in the previous paper by Pegalajar-Jurado et al. (2018)). We have added a sentence, see P4L23, to make this more clear.

RC: The ultimate nacelle accelerations are underpredicted in QuLAF, whereas the ultimate tower-base bending moments agree well. Often, accelerations are more sensitive to higher modes than ultimate bending moments. I did not find information on the number of tower modes used in FAST for this application. If it uses more than one tower mode, the following comment may be relevant: In addition to the underprediction of the wave excitation loads for strong sea states due to the omission of viscous hydrodynamic drag forcing, could the omission of the second tower mode in QuLAF also be part of the explanation? One way to examine this would be to turn off modes two and higher in FAST, or look at the response-spectra from FAST. Please include information on the number of tower modes used in FAST, and, under model limitations for QuLAF, mention that only first tower bending modes are used. Have any sensitivity studies on the number of tower modes ben carried out?

AC: The number of tower modes in FAST has been added now, see P3L8. Regarding the effect of the higher tower modes, we checked the response, where mode two and higher in FAST were turned off. This only had very minor impact on the nacelle acceleration, thus we believe the under-prediction of the nacelle acceleration is due to the over-estimated damping of the tower mode.

RC: The aerodynamic damping model seems to be one area where changes could significantly improve the results. One possible improvement would be to perform the decay test in FAST with flexible blades, resulting in an eigen frequency closer to the coupled tower frequency in QuLAF, thereby reducing the over-prediction of aerodynamic damping. It should also be possible to have an aerodynamic damping model in QuLAF model derived directly from a linearized BEM model.

AC: We thank the referee for the ideas of improvement. We are already exploring better ways to extract the aerodynamic damping. The results, however, are still not mature. Inclusion of flexible blades could also lead to an improvement, but introduces choices as to what specific mode one should choose (blades in phase (anti-phase etc.)). We have chosen to stay with the current simple approach and simply accept its limitations.

RC: I find it quite surprising, interesting and perhaps under-communicated that an emergency stop can be successfully computed with a frequency domain model. More details, such as direct comparison of the time series of tower base bending moments and nacelle accelerations would be very welcome.

AC: We agree, it is very interesting that QuLAF is able to reproduce a transient event and thank the referee for the suggestion of improvement to this comparison. We have added a figure showing the time series of a specific case in the discussion of DLC2.1, see Figure 7, page 16.

RC: Page 4, line 14: Did you check that there is no numerical damping in the decay test? One way to test this is to scale down the lift-and drag coefficients, or somehow provide an excitation of the tower top without rotor aerodynamics present.

AC: Regarding the numerical damping, we did a clamped pre-study of the model in 0 m/s and forced excitations of the tower top. The study showed that the response was undamped, i.e. no numerical damping present.

Please note that other minor changes have been introduced in the text to improve readability and fix a few typos.

Performance study of the QuLAF pre-design model for a 10MW floating wind turbine

Freddy J. Madsen[1], Antonio Pegalajar-Jurado[1], and Henrik Bredmose[1]

[1]Department of Wind Energy, Technical University of Denmark, Nils Koppels Allé, Building 403, DK-2800 Kgs. Lyngby, Denmark

Correspondence: Freddy J. Madsen (fjma@dtu.dk)

Abstract. This paper presents a comparison study of the simplified model QuLAF (Quick Load Analysis of Floating wind turbines), and a FAST model of the DTU 10MW Reference Wind Turbine mounted on the LIFES50+ OO-Star Wind Floater Semi 10MW floating substructure. The purpose is to investigate how accurate results can be obtained from this simplified model for different load cases. The two models are briefly presented and the limitations of QuLAF are discussed. These are (A) an under-prediction of the wave excitation loads for large sea states; (B) a simplified representation of the rotor-induced forcing and damping; (C) an over-predicted aerodynamic damping for the tower mode motion and (D) restriction to planar motion. All the limitations are linked to approximations applied for achieving the substantial model speed up relative to the state-of-the-art model. The comparative study is based on the planar version of design load cases (DLC) 1.2, 1.3, 1.6, 2.1 and 6.1 and the overall analysis shows that the simplified model is generally ~~very~~ good at estimating the bending moment at the tower base and the floater motions in heave and pitch. The largest tower-base bending moments are slightly over-predicted, but it is observed that while stronger wind leads to an over-prediction, stronger waves lead to an under-prediction. Thus in DLC 1.6, where the largest load was obtained at 10.3 m/s, a ~~perfect~~ good match in tower base bending moments between the two models is found. The nacelle acceleration, however, is generally under-predicted, which is ~~likely due~~ linked to an over-prediction of the aerodynamic damping on the tower mode. Furthermore the floater response in large sea states is influenced by the omission of viscous hydrodynamic drag forcing, which leads to an under-prediction of the wave excitation loads. A further investigation of the model limitations confirms these findings with respect to the tower mode damping and viscous drag loads, while the simplified approach to rotor-induced loads is found to provide remarkable accurate forcing results. Although a full design load basis evaluation with a state-of-the-art model must be carried out for the final design, the present results show the potential of applying ~~the QuLAF model~~ simplified models in the preliminary design phase.

1 Introduction

The design of floaters for offshore wind turbines usually follows three steps: Conceptual design, basic design, and detailed design. Within basic design, state-of-the-art models such as FAST, Bladed or HAWC2 are used to calculate time-domain loads under various design load cases. As described in Müller et al. (2018), load cases are an inherent part in the wind turbine standards and define the specific design load criteria for the structural design according to defined classes of environmental conditions. These generic conditions describe wind, waves, gusts, currents, etc. and their related meteorological parameters in different classes of severity. The goal of conducting load cases is to cover all relevant load situations within the designated life time of the structure, but more importantly to cover all potential design-driving situations, i.e. the situations leading to critical design loading. Load cases consist of normal operation, extreme events, stand-still conditions and transient events such as start-up, shut-down, and fault conditions.

Conducting a full design load basis (DLB) analysis, consisting of all design load cases for a floating wind turbine design for several concepts, is computationally expensive, especially if they are carried out with time-domain numerical tools simulating at real-time CPU speed ~~.~~ (i.e. a simulated-to-simulation ratio of 1). Faster models, may thus be valuable in the conceptual design phase, where quick answers for response levels and load levels may affect the design at an early stage. Also the accuracy requirements may be relaxed and allow for application of low-dimensional models enabling the application of optimization methods. Next, when the concept design is more ~~converged~~refined , state-of-the-art models can be used in the design validation following current practice; and eventually more advanced models can be used for detailed design tasks. For certification, loads analysis of the full set of design load cases according to recognized standards using state-of-the-art models is required.

The present study concerns the applicability of simplified models in the design of floaters for offshore wind turbines in the 10MW class, in order to answer the following question: *how accurate results can be obtained from simplified models for different load cases?* The work is part of the Lifes50+ project where both a state-of-the-art FAST model (Pegalajar-Jurado et al., 2018b),(Pegalajar-Jurado et al., 2018c) and a simplified model (Pegalajar-Jurado et al., 2018a) have been developed.

The simplified model QuLAF (Quick Load Analysis of Floating wind turbines) is based on the same principles as the QuLA model of Schløer et al. (2018) for mono-pile type offshore wind turbines. First, in Section 2, the wind turbine, controller and the floating substructure are briefly described. Details on the FAST model and the simplified QuLAF model are given in Section 3. In Section 4 a selection of load cases is presented and the simulation setup described. Results of the simulations are shown in Section 5, along with a discussion of the observed trends. In continuation of the main results, Section 6 presents an investigation of QuLAF's limitations, focussing on how they affect the response of the structure. Lastly, some conclusions of the study are presented in Section 7.

2 Wind turbine and floating substructure

The floating wind turbine is the DTU 10MW RWT (Bak et al., 2013) mounted on the OO-Star Wind Floater Semi 10MW, extensively described in Yu et al. (2018). Some of the main properties of the reference wind turbine are collected in Table 1.

The basic DTU Wind Energy controller is employed (Hansen and Henriksen, 2013), which consists of a controller for the partial load region (i.e. operation below rated wind speed) and one for the full load region (i.e. operation above rated wind speed), and a mechanism that smoothly switches between these around rated wind speed. The pole-placement method, described in Hansen et al. (2005), was used to tune the controller to avoid pitch instability, as detailed in Yu et al. (2018).

The floating substructure, developed by Dr.techn. Olav Olsen AS (http://www.olavolsen.no) is made of post-tensioned concrete and consists of a central column and three outer columns mounted on a star-shaped pontoon with three legs. Each outer

Table 1. Main properties of the DTU 10MW reference wind turbine.

Rated power [MW]	Rated wind speed [m/s]	Wind regime	Rotor diameter [m]	Hub height [m]
10	11.4	IEC Class 1A	178.3	119

column is connected to the seabed by a catenary mooring line with a suspended clump weight. Some of the main properties of the floater configuration are stated in Table 2 and further information can be found in Yu et al. (2018).

Table 2. Main properties of the OO-Star Semi floating substructure.

Type	Material	Draft [m]	Freeboard [m]	Displaced volume [m^3]	Floating substructure mass [kg]
Semisubmersible	Post-tensioned concrete	22.00	11.00	$2.351 \cdot 10^4$	$2.171 \cdot 10^7$

3 Numerical models

3.1 State-of-the-art model

A FAST (Jonkman and Jonkman, 2016) time-domain model of the DTU 10MW RWT mounted on the OO-Star Wind Floater Semi 10MW has been developed in the LIFES50+ and reported in Pegalajar-Jurado et al. (2018b) and Pegalajar-Jurado et al. (2018c). A semi-flexible approach has been adapted in the modelling work to capture some of the floating substructure flexibility by extending the definition of the tower to still water level (SWL) (Pegalajar-Jurado et al., 2018b). Two tower modes are included in each direction (fore-aft and side-side).

The hydrodynamic modelling is based on pre-computed linear radiation-diffraction coefficients, obtained by the frequency-domain, potential-flow solver WAMIT (Lee and Newman, 2016). No second-order effects were included in this study. Viscous drag is not captured by potential-flow solvers, thus it is included by the drag term in the Morison equation. Since FAST allows only cylindrical members of the floater for the Morison description, special efforts was made to represent the effect of the heave plates in both surge/sway, heave and pitch/roll. This is detailed in Pegalajar-Jurado et al. (2018b). Finally the model utilizes a dynamic lumped-mass mooring line model that allows the use of multi-segmented mooring lines.

3.2 The simplified model: QuLAF

A simplified model of the floater-turbine configuration was implemented in terms of the QuLAF model. The modelling concept and philosophy is described in Schløer et al. (2018) for bottom-fixed substructures and in Pegalajar-Jurado et al. (2018a) for floating wind turbines, see also Lemmer et al. (2016). The main purpose of QuLAF is to provide quick answers about design loads and natural frequencies in the pre-design phase, where many design variations are tried before the first basic design is chosen. The simplicity and efficiency is obtained by inclusion of only four degrees of freedom, linearization of the equations of motion, pre-computation of aerodynamic rotor forcing and damping, and solution of the equations of motion in the frequency domain. As a result of these simplifications, the computational speed in QuLAF is approximately 2000 times faster than real time (after pre-processing of the aerodynamic loads), whereas standard time-domain models have a simulated-to-real time ratio around 1.

The four degrees of freedom are the platform surge, heave and pitch and the modal amplitude of the first tower mode, which is illustrated in Figure 1. Thus QuLAF solves only a 2D problem and is restricted to aligned wind and waves. For the load predictions, this means that only the fore-aft moments and forces can be considered. The linear equations of motion in the frequency domain are written in QuLAF as (1), considering the three in-plane floater degrees of freedom and the flexible tower mode as a fourth degree of freedom.

$$\left[-\omega^2\left[\mathbf{M}_{str}+\mathbf{A}(\omega)\right]+i\omega\left[\mathbf{B}_{rad}(\omega)+\mathbf{B}_{visc}+\mathbf{B}_{aero}+\mathbf{B}_{str}\right]+\left[\mathbf{C}_{hyd}+\mathbf{C}_{moor}+\mathbf{C}_{str}\right]\right]\hat{\mathbf{x}} = \hat{\mathbf{F}}_{aero}+\hat{\mathbf{F}}_{hyd}. \tag{1}$$

Here ω is the angular frequency, $\mathbf{x}=[\xi_1,\xi_3,\xi_5,\delta]^T$ is the response vector, $\mathbf{M}_{str}$ is the structural mass matrix, $\mathbf{B}_{str}$ is the structural damping, $\mathbf{C}_{str}$ is the structural stiffness and $\mathbf{F}_{hyd}$ are the hydrodynamic loads. The aerodynamic loads $\mathbf{F}_{aero}$ are pre-computed with fixed nacelle, rigid blades and active control. The matrices $\mathbf{A}(\omega)$, $\mathbf{B}_{rad}(\omega)$ and $\mathbf{C}_{hyd}$ are the hydrodynamic added mass, hydrodynamic radiation damping and the hydrostatic stiffness, which are obtained from the WAMIT solver. The mooring restoring matrix $\mathbf{C}_{moor}$ is extracted from the state-of-the-art model by linearization around each equilibrium position, i.e. for each mean wind speed. In QuLAF, the viscous forcing is neglected, while the viscous damping $\mathbf{B}_{visc}$ is represented by a linearized damping matrix under the assumptions of inertia load dominance and small amplitude motion. More details are given in Pegalajar-Jurado et al. (2018a). It should be noted that damping on the mooring lines is not included in QuLAF, but for floaters where this is important, this can be included in the global damping matrix.

A state-of-the-art model, which in this study is the FAST model, is used to provide inputs to QuLAF, such as the simplified structural tower modelling, the aerodynamic forcing and damping and the linearized mooring matrix. This means that QuLAF contains phase information, as time-series of pre-computed aerodynamic loads and free-surface elevation are input to the model. As a consequence, time-series of the results are available for comparison to time-domain models and for further post-processing, such as rainflow counting.

The linear representation of the aerodynamic damping $\mathbf{B}_{aero}$ is obtained from step tests in steady wind, where the wind speed goes from the cut-in to the cut-out. This means that for every step to a new wind speed, the structure decays to a new equilibrium position. These "decays" allows an equivalent linear damping ratio to be extracted and the principle is based on the work done by Schløer et al. (2016), Schløer et al. (2018). Schafhirt and Muskulus (2018) made a detailed analysis of this approach and found that although the aero-elastic damping process is not linear, it can be successfully modelled by a linear damping model. In QuLAF, the approach is extended to multiple degrees of freedom. These decay tests are carried out in the FAST model in calm water and with the wind turbine controller active, for each degree of freedom with all the other degrees-of-

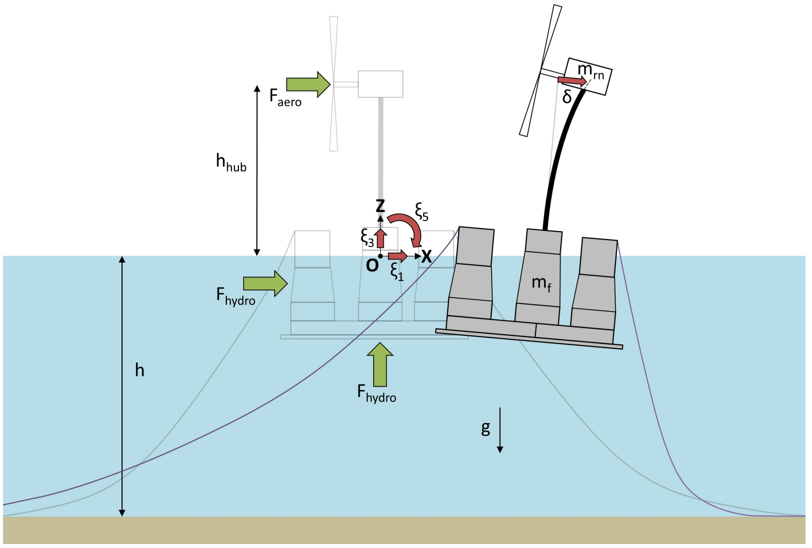

Figure 1. Sketch of the floating wind turbine as seen by the QuLAF model. From Pegalajar-Jurado et al. (2018a).

freedom locked and rigid blades. This ~~allow~~ allows the floating wind turbine to be a one degree of freedom spring-mass-damper system in each degree of freedom, where the horizontal position of the hub is of interest.

If all sources of hydrodynamic and structural damping are disabled, the aerodynamic damping is the only responsible for the decay of the hub motion, and it can be extracted from the time series. For simplicity, the turbulence intensity was put to zero to limit the number of decay tests.

3.3 Summary of model limitations

QuLAF solves a linear and reduced version of the equations of motion typically solved in a full state-of-the-art model, to allow for the linearization and fast solution in the frequency domain. Prior to the present study, a smaller set of results with the QuLAF model has been presented in Pegalajar-Jurado et al. (2018a). In Pegalajar-Jurado et al. (2018a) and the present results, the main limitations of QuLAF were summarized as:

A. An under-prediction of the wave excitation loads for strong sea states due to the omission of viscous hydrodynamic drag forcing. This leads to an under-prediction of surge, nacelle acceleration and pitch responses for strong sea states.

B. Difficulty to capture the complexity of aerodynamic loads around rated wind speed, where the controller switches between the partial-load (torque control; fixed blade pitch) and full-load control regions (varying blade pitch; fixed target shaft speed).

C. An under-predicted nacelle acceleration due to over-predicted aerodynamic damping for the tower mode motion (at 0.682 Hz). Since the damping of the decay test, used to extract the aerodynamic damping, is based on a clamped tower with rigid blades, the natural frequency of this setup (0.51 Hz) is lower and thus leads to a larger damping than that at the coupled tower frequency in QuLAF (0.682 Hz). In comparison, the full FAST model has a coupled tower frequency of 0.746 Hz when moored and with flexible blades.

4 Load cases

The present study shows the mapping of accuracy between the simplified model QuLAF (Pegalajar-Jurado et al., 2018a) and the FAST model for a subset of critical load cases, which are selected based on the findings from Müller et al. (2018). The selected load cases included fatigue during normal operation (DLC 1.2), ultimate loads during power production in severe sea states (DLC 1.6) and ultimate loads when the turbine is parked during a 50-year storm event (DLC 6.1). Further, for the present study of analysing the applicability of QuLAF in the design phase, it was decided to add two additional design load cases, namely ultimate loads during power production in extreme turbulence (DLC 1.3) and ultimate loads during a transient event triggered by a loss of electrical network connection (DLC 2.1). DLC 1.3 was considered in order to fully evaluate the results of QuLAF by comparing with the baseline load case (DLC 1.2) and the extreme sea state load case (DLC 1.6). DLC 2.1 was included to see how well QuLAF handles a transient event.

Table 3 details the selection of load cases as stated in the IEC61400-3 design code (61400-3, 2009). Here NTM, ETM and EWM refer to normal turbulence model, extreme turbulence model and extreme wind model. Further NSS, SSS and ESS refer to normal, severe and extreme sea state. Simplifications have been made to each load case since QuLAF only solves a 2D problem and is thus restricted to aligned wind and wave load conditions. This also means that only in-plane loads and motions has been investigated. All NSS load cases were based on the long term joint probability distribution of metocean parameters presented in Krieger et al. (2015), which were to be considered for the fatigue analysis. Ideally, one would use the site-specific data for the other DLCs with NSS, but in order to have DLC 1.2 to also serve as a baseline load case for the ultimate limit state (ULS) DLCs it was decided to use the joint probability distribution NSS. In agreement with the project design basis (Krieger et al. (2015)), each wind speed in each load case had three realisations of the wave spectrum peak period.

Six different wind and wave seeds were simulated for each environmental condition, with the only exception of DLC 2.1 where four seeds were deemed sufficient, as the maximum loads in this case are governed by the transient shut-down event. For each environmental condition, the characteristic value is the mean of the maximum values of the different realizations (seeds) and is used for evaluation. Furthermore, a simulation time of 5400s with the same length of turbulent wind field was used for all the load cases including 1800s run-in-time to remove any transient response in the time-domain model. This run-in-time corresponds to approximately 9 surge periods, which was deemed acceptable for the lowest sea state, where the transient influence is highest.

Table 3. Selection of design load cases. Note that the comparative study was limited to aligned wind-wave conditions only, due to the restriction of QuLAF to planar motion. Each simulation had a length of 90 min, where the first 30 min were discarded to remove transient response in the time-domain model.

Load case	Description	Environmental conditions		Number of simulations
		Wind	Waves	
DLC1.2	Power production during normal operation	NTM $V_{in} < V_{hub} < V_{out}$	NSS Joint prob. Distribution of H_s, T_p, V_{hub}	(7 wind speeds) ×(3 wave periods) ×(6 seeds)
DLC1.3	Power production during extreme turbulence	ETM $V_{in} < V_{hub} < V_{out}$	NSS $H_s = (H_s \vert V_{hub})$	(7 wind speeds) ×(3 wave periods) ×(6 seeds)
DLC1.6	Power production during severe sea states	NTM $V_{in} < V_{hub} < V_{out}$	SSS $H_s = H_{s,SSS}$	(7 wind speeds) ×(3 wave periods) ×(6 seeds)
DLC2.1	Power production with grid loss	NTM $V_{in} < V_{hub} < V_{out}$	NSS $H_s = (H_s \vert V_{hub})$	(7 wind speeds) ×(3 wave periods) ×(4 seeds)
DLC6.1	Parked in extreme wind and sea state	EWM $V_{hub} = V_{ref,50y}$	ESS $H_s = H_{s,50y}$	(1 wind speed) ×(3 wave periods) ×(6 seeds)

5 Results

The results involve a fatigue limit state (FLS) analysis and an ultimate limit state (ULS) analysis, each displaying the design load and response values for different parts of the floating wind turbine, i.e. nacelle acceleration, tower-base bending moment, surge, heave and pitch motion of the floater.

In general the design load and response values for both the QuLAF model and the FAST model are presented as function of wind speed. Thus the wave heights and periods were chosen according to the wind speed, as specified in Table 3 and in Krieger et al. (2015). In addition, to better compare the load prediction of the two models, corresponding quantile-quantile (Q-Q) plots are also presented. Furthermore at the end of Section 5, box-plots of the response peaks are used to describe the spread and median of the ratio between the damage-equivalent or maximum values from QuLAF and FAST.

5.1 FLS study

First we present the results of the fatigue evaluation study. In the analysis, the damage-equivalent loads (DELs) are presented, computed from each load time series by the rainflow counting method. Although the nacelle acceleration is not a load, it was analysed with the rainflow counting method and presented as DEL, since internal loads in the nacelle may be directly related to the nacelle acceleration. The fatigue DEL nacelle acceleration and tower-base bending moment for FAST and QuLAF are shown in Figure 2 as function of wind speed, together with the corresponding Q-Q plot.

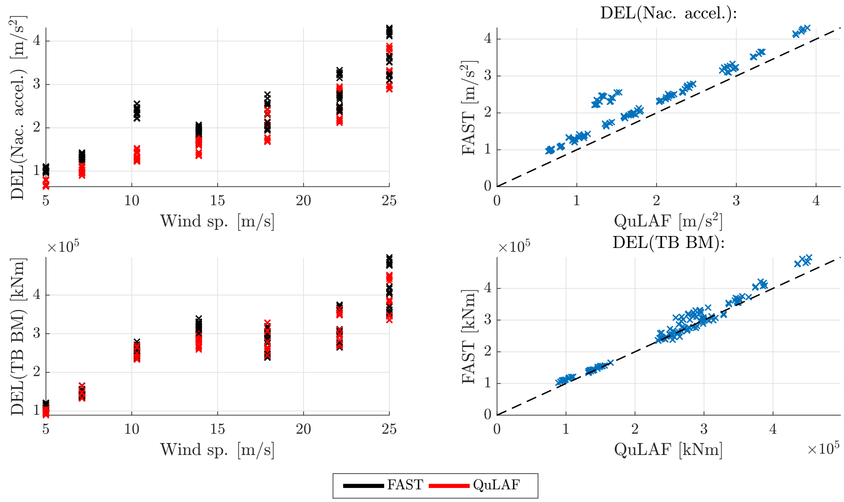

Figure 2. Fatigue damage-equivalent nacelle acceleration and bending moment at the tower-base for DLC1.2.

These results are followed by Table 4 presenting the DEL values, where the weighting of the different wind speeds and ~~peak~~ wave periods according to the assumed Weibull distribution and probabilities (Krieger et al., 2015), has been taken into account.

Table 4. FAST and QuLAF probability-weighted DEL results, based on probabilities from the Weibull distribution of NSS [7].

	FAST	QuLAF	ratio
DEL: Nac. accel. [m/s^2]	1.86	1.38	0.74
DEL: TB BM [kNm]	$2.29 \cdot 10^5$	$2.18 \cdot 10^5$	0.95

It can be seen that the nacelle acceleration is generally under-predicted in QuLAF and since the nacelle acceleration is governed by the wind forcing for this load case, it might be explained by an enhanced effect of limitation B (the complex dynamics around rated conditions makes the controller behave differently in the two models) and C (the over-estimated aerodynamic damping on the tower vibrations in QuLAF). This may also explain the distinct deviation at 10.3m/s, which is highly affected by the controller transition. The largest DEL for both models is observed at the strongest environmental state, i.e. 25 m/s, but with a 20% under-prediction in QuLAF. However the largest DEL contribution is associated with rated conditions when the probabilities from the Weibull distribution is taken into account.

The tower-base bending moment, on the other hand, shows ~~a~~ an overall good agreement between the two models, but with a slight under-prediction of QuLAF just above rated conditions and at cut-out. A conclusion that can also be observed in Table 4, for the total Weibull-weighted DEL. It is seen that, while ~~QuLAF under-predicts~~ a disagreement is seen for the nacelle acceleration DEL ~~by~~ (an under-predicts of 26%), the tower-base bending moment agrees well, with an under-prediction ~~is only~~ of 5%.

5.2 ULS study for operational load cases

We now proceed with the ULS simulation study for the operational load cases. A total of ~~18~~ 126 1-hour ~~realizations with~~ simulations (7 wind speeds $\times$ 3 wave periods $\times$ 6 seeds) were carried out for each of the two models~~were carried out~~. Although DLC 1.2 (power production in normal conditions) is intended for fatigue analysis, we present ULS results from this load case as well, to form a baseline for DLC 1.3 and DLC 1.6 with stronger turbulence and waves, respectively.

Figure 3 shows the nacelle acceleration, tower-base bending moment and floater motion across the various wind speeds for the two models. Overall, there is a good ~~match~~ agreement between the models, especially for the floater motion (5% mean deviation of the max. values), even at large values of response, and it is seen that all but the heave motion are wind-dominated. Similarly to the FLS study, the nacelle acceleration is under-predicted by QuLAF and the largest value is obtained at 25 m/s with an 11% under-prediction, as seen in Table 5. The largest under-prediction is observed around rated conditions and may be linked to limitation B. It is also seen that QuLAF also over-predicts the tower-base bending moment for the largest values obtained around rated conditions by 7-13%.

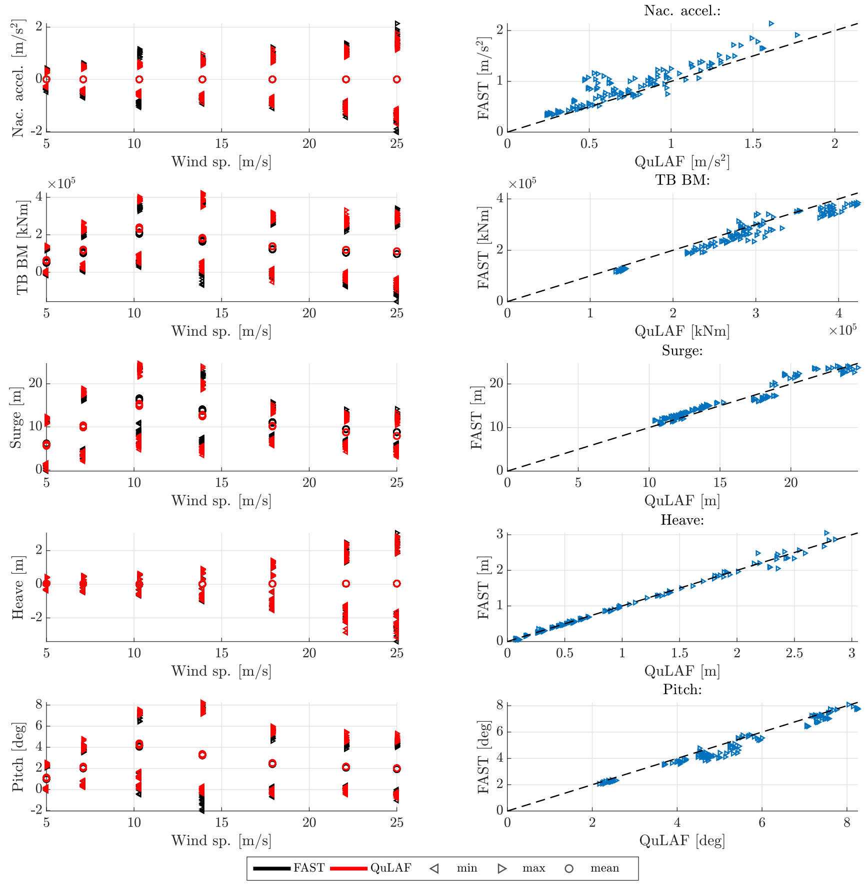

Figure 3. Response to DLC1.2 for FAST and QuLAF. Left: min., max. and mean values for every realisation as function of wind speed. Right: maximum values for FAST as function of the corresponding maximum values in QuLAF

Table 5. ~~Mean values~~ Ratio of ~~the response ratios of the~~ max. ~~values~~ response (QuLAF/FAST) averaged per wind speed for DLC1.2.

Mean(~~X_{Qulaf}/X_{FAST}~~ $X_{Qulaf,max}/X_{FAST,max}$) [−]	Wind speed [m/s] 5.0	7.1	10.3	13.9	17.9	22.1	25.0
Nac. Accel.	0.75	0.88	0.57	0.94	0.90	0.89	0.89
TB BM	1.12	1.14	1.13	1.07	1.08	1.11	1.00
Surge	0.99	1.08	0.99	0.95	0.94	0.94	0.93
Heave	1.01	1.06	1.15	1.01	1.01	1.02	0.99
Pitch	1.07	1.08	1.05	1.02	1.05	1.14	1.10

We can now turn to DLC 1.3 which consists of the same number of realizations simulations as for DLC 1.2, but now with extreme turbulence. In Figure 4 the nacelle acceleration, tower-base bending moment and planar motions of the floater are shown as function of mean wind speed together with the corresponding Q-Q plot.

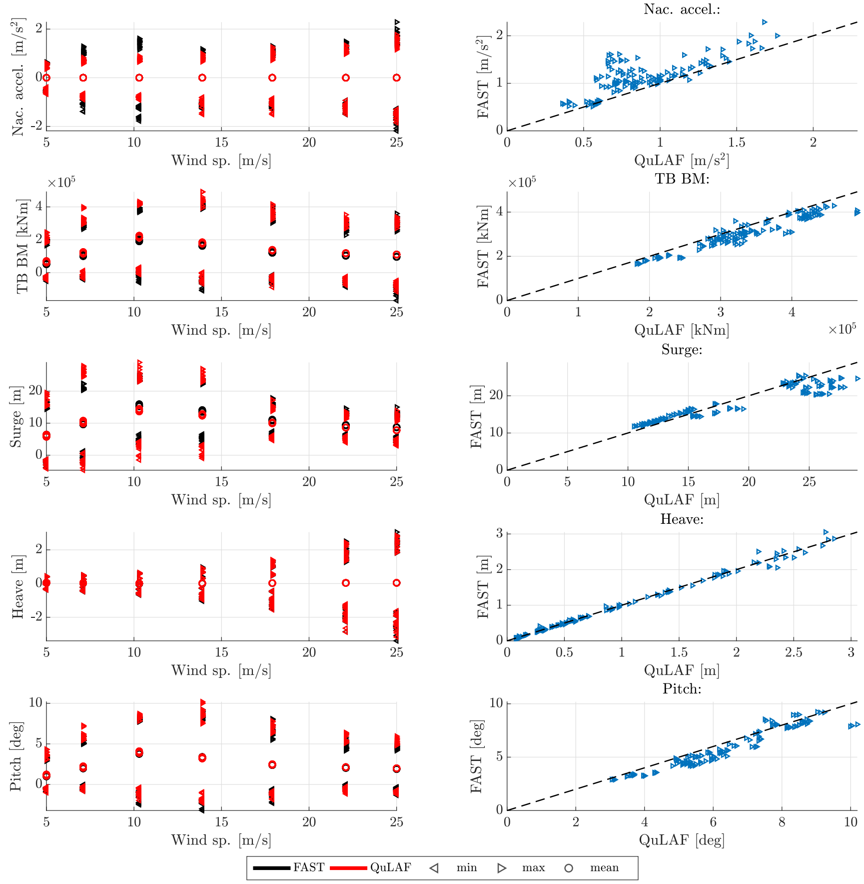

Figure 4. Response to DLC1.3 for FAST and QuLAF. Left: min., max. and mean values for every realisation as function of wind speed. Right: maximum values for FAST as function of the corresponding maximum values in QuLAF

Overall the wind forcing is more dominant for low wind speeds when compared to DLC 1.2. However the load variation trend is similar to DLC 1.2, where the largest values of response is seen around rated wind speed for the tower-base bending moment, surge and pitch, while the nacelle acceleration and heave is largest at 25 m/s. The extreme turbulence enhances the relative surge and pitch response in QuLAF. This can be seen as a large over-prediction in surge and pitch at 7.1 m/s of 22% and 13% respectively, while an 44% under-prediction of the nacelle acceleration is also observed. The largest nacelle acceleration is obtained at rated conditions with a severe under-prediction of 47%, as seen in Table 6. As for DLC 1.2 the tower-base bending moment shows the largest load at rated conditions, with the same level of over-prediction of 11%. Similarly, for For the heave motion the responses from the two models agree very well (mean deviation of 3%) and are largest at cut-out.

Table 6. Mean values Ratio of the response ratios of the max. values response (QuLAF/FAST) averaged per wind speed for DLC1.3.

Mean(X_{Qulaf}/X_{FAST} $X_{Qulaf,max}/X_{FAST,max}$) [−]	Wind speed [m/s] 5.0	7.1	10.3	13.9	17.9	22.1	25.0
Nac. Accel.	0.88	0.66	0.53	0.80	0.91	0.93	0.87
TB BM	1.13	1.14	1.11	1.09	1.08	1.14	1.04
Surge	1.10	1.22	1.03	1.07	0.94	0.93	0.92
Heave	1.03	1.10	1.04	0.98	1.01	1.02	1.00
Pitch	1.13	1.13	1.04	1.03	1.06	1.17	1.16

For DLC 1.6, the waves are given by the severe sea state, which for the given design basis correspond to the 50-year sea state, while the turbulence model is normal as in DLC 1.2. This means that the same severe waves are applied across all wind speeds. Thus only six realizations are consideredconsisting of the same number of simulations as for DLC 1.2 and DLC 1.3 (7 wind speeds × 3 wave periods × 6 seeds). The nacelle acceleration, tower-base bending moment and planar motions of the floater are shown in Figure 5 as function of mean wind speed together with the corresponding Q-Q plot. Furthermore Table 7 describes the mean values of the response ratios.

Compared to DLC 1.2, the nacelle acceleration and tower-base bending moment are now more wave-dominated, as the max response values are more uniform over the wind speeds due to the fact that severe waves are the same across all wind speeds. It is seen that nacelle acceleration is generally under-predicted up to 25%, which may be due to limitation A and C. However the largest tower-base bending moments, obtained at rated wind, is matched perfectly very well by QuLAF. This good match is unexpected, given the observed discrepancies for extreme-waves and extreme-wind situations for the present floater, and it is probably due to a cancellation effect.

The floater motions, with respect to surge and heaveare matched very well between the two models, with a 7-8% under-prediction , shows a good agreement around rated for surge and overall with a 7-8% under-prediction and overall a very good match for heave, where an under-prediction of 3% for the heave. is observed. The consistent under-prediction of the surge response by QuLAF, seen in Table 7, is linked to limitation A (omission of the viscous hydrodynamic drag forcing), but could be a mix A and C (QuLAF over-estimates the aerodynamic damping on the tower vibrations) around rated. Furthermore it can be observed for the surge motion, that the combination of larger waves and under-prediction in DLC 1.2 and DLC 1.3 compensates the deviation between QuLAF and FAST for the largest responses, which might be linked to limitation A.

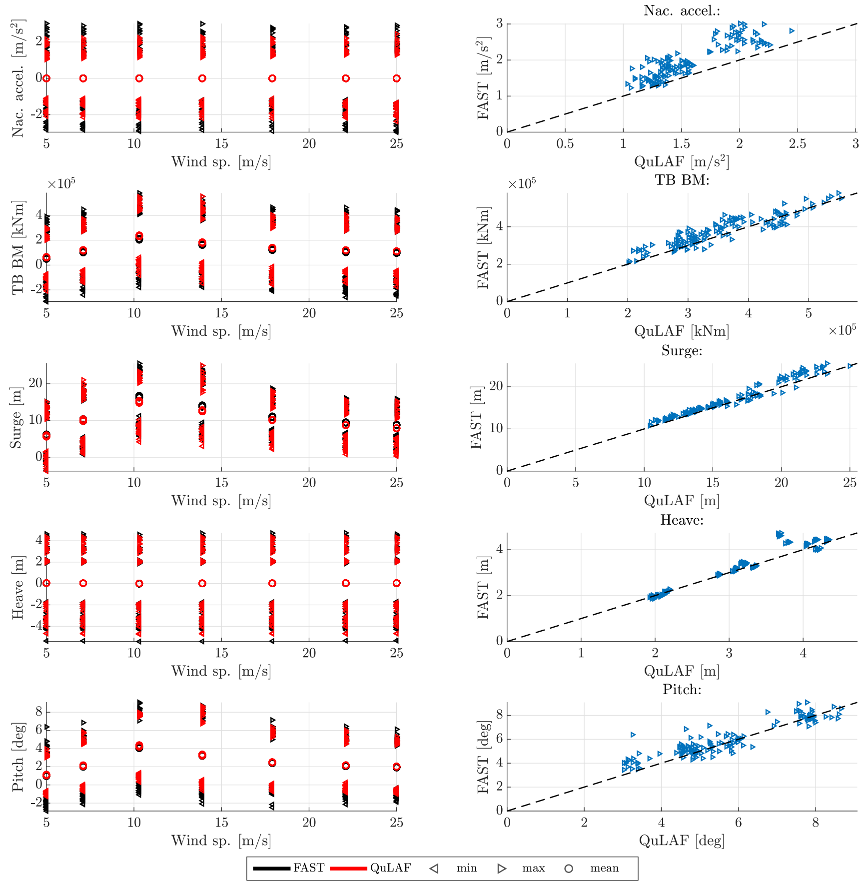

Figure 5. Response to DLC1.6 for FAST and QuLAF. Left: min., max. and mean values for every realisation as function of wind speed. Right: maximum values for FAST as function of the corresponding maximum values in QuLAF

Table 7. ~~Mean values~~ Ratio of ~~the response ratios of the~~ max. ~~values~~ response (QuLAF/FAST) averaged per wind speed for DLC1.6.

Mean(~~X_{Qulaf}/X_{FAST}~~ $X_{Qulaf,max}/X_{FAST,max}$)	Wind speed [m/s]						
[−]	5.0	7.1	10.3	13.9	17.9	22.1	25.0
Nac. Accel.	0.75	0.75	0.77	0.84	0.83	0.82	0.84
TB BM	0.85	0.92	1.00	1.01	0.93	0.94	0.91
Surge	0.96	1.03	0.92	0.93	0.95	0.95	0.93
Heave	0.97	0.97	0.98	0.97	0.97	0.98	0.97
Pitch	0.80	0.92	0.97	1.00	0.99	0.98	0.97

5.3 ULS study for grid loss and parked conditions

We now proceed with the ULS simulation study for grid loss and parked conditions. The former This load case is included to demonstrate that even for a transient event, the frequency-domain approach is applicable. In all simulations, an emergency stop at $t = 3600$ s was simulated during operation with normal turbulence and normal sea state. A total number of 12 realizations (i.e. four 84 simulations (7 wind speeds $\times$ 3 wave periods $\times$ 4 seeds) are considered, where only four seeds are included as the transient event governs the maximum loads and responses.

The nacelle acceleration, tower-base bending moment and planar motions of the floater are shown in Figure 6. Overall we see that QuLAF does a good job in handling the transient load case when compared to the FAST results. Also it can be seen that the load and response variation trend is very similar to DLC 1.2 . The deviation levels in Table 8 and from Table 8 the deviation levels on the maximum values are of the same magnitudeand the reason for this is that only maximum values have been considered in the table. This might not be representative for .

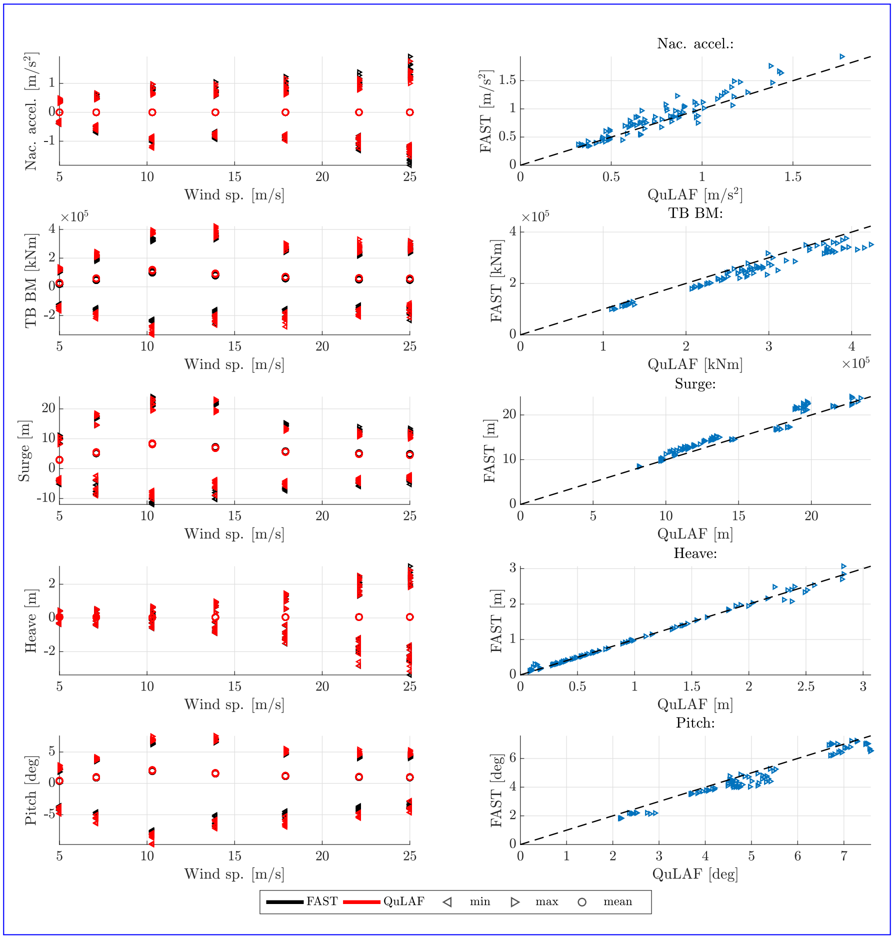

Figure 6. Response to DLC2.1 for FAST and QuLAF. Left: min., max. and mean values for every realisation as function of wind speed. Right: maximum values for FAST as function of the corresponding maximum values in QuLAF

By inspection of the left column of Figure 6, the negative extreme values are of the same importance as the extreme positive in this transient load case~~, where also the negative values have high influence, as can be seen in the left columnof Figure 6.~~. Thus the deviation levels on the minimum values are also included in Table 8. Generally it is seen that higher deviation levels are obtained for the minimum response ratios compared to the maximum. The largest deviations are seen for the surge motion for wind speeds greater than 5 $\mathrm{m/s}$. This is further investigated by examination of the corresponding time series, as seen in Figure 7. We chose the case with a mean wind speed of $13.9\,\mathrm{m/s}$, as it is close to rated wind speed where the largest bending moments occur. At this wind speed the time series for the 12 simulations (3 wave periods $\times$ 4 seeds) are shown in grey. Further, their average is shown in blue and red for FAST (first column) and QuLAF (second column) respectively. The right column show a direct comparison of the averaged signals.

~~Response to DLC2.1 for FAST and QuLAF. Left: min., max. and mean values for every realisation as function of wind speed. Right: maximum values for FAST as function of the corresponding maximum values in QuLAF~~

Table 8. ~~Mean values~~ Ratio of ~~the response ratios of the~~ max. ~~values~~ and min. response (QuLAF/FAST) averaged per wind speed for DLC2.1.

Mean(~~X_{Qulaf}/X_{FAST}~~ $X_{Qulaf,max}/X_{FAST,max}$)	Wind speed [m/s]						
[−]	5.0	7.1	10.3	13.9	17.9	22.1	25.0
Nac. Accel.	1.00	0.99	0.91	0.94	0.93	0.90	0.88
TB BM	1.10	1.13	1.15	1.08	1.08	1.15	1.06
Surge	0.96	1.04	0.93	0.92	0.90	0.91	0.89
Heave	0.93	0.92	0.86	1.01	1.01	1.02	0.99
Pitch	1.17	1.06	1.07	1.02	1.07	1.14	1.09
Mean($X_{Qulaf,min}/X_{FAST,min}$) [−]							
Nac. Accel.	0.97	0.94	1.02	0.91	0.98	0.98	0.91
TB BM	1.15	1.21	1.26	1.15	1.28	1.20	0.93
Surge	0.90	0.79	0.78	0.68	0.77	0.81	0.77
Heave	1.92	0.72	0.84	0.95	0.99	1.03	0.99
Pitch	1.08	1.11	1.10	1.07	1.21	1.22	1.05

From the figure it can be concluded that QuLAF captures the decay after shut-down very well with except for a pronounced deviation in the surge motion. This is likely due to the surge mooring stiffness not being "updated" in QuLAF. Physically, after the shutdown the structure goes back to the equilibrium position due to the restoring effects. In FAST the mooring system is represented by a dynamic mooring model, which includes nonlinear effects and thus takes into account the reduction in surge stiffness as the floater moves back to the equilibrium position. In QuLAF, on the other hand, the mooring matrix used in this case is the one for the given wind speed (13.9 m/s), which represents well the stiffness at that operating point but differs from the stiffness matrix at the equilibrium position. Thus in QuLAF, the system decays with a stiffer mooring system, which is consistent with the shorter surge natural period observed in Figure 7. This is an inherent limitation of frequency-domain models, which do not allow the system properties to change during the simulation.

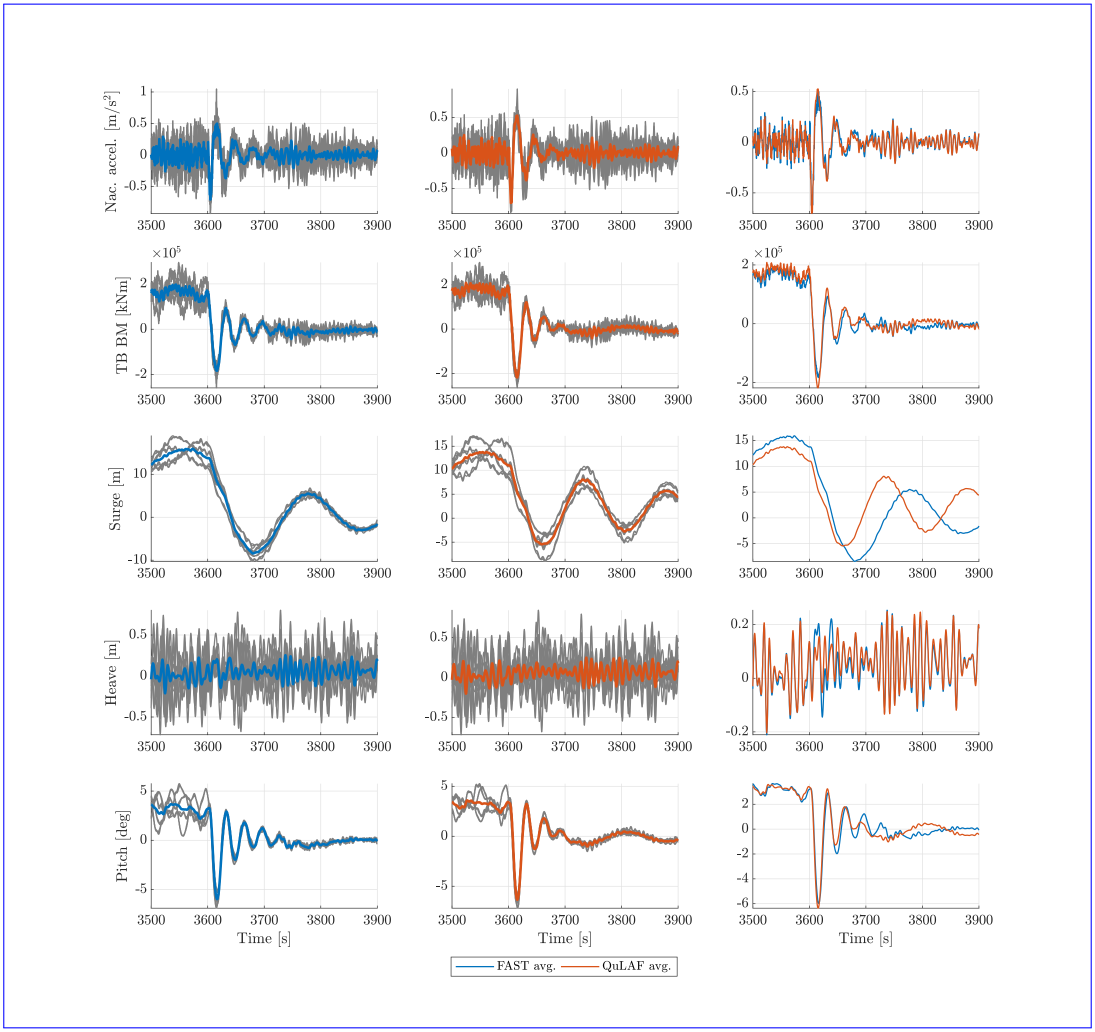

Figure 7. Zoomed time series of DLC2.1 with a mean wind speed of 13.9 m/s for FAST and QuLAF. The average responses are obtained based on the four different wave and wind seeds and three realization of the peak period.

We can now turn to DLC 6.1 which describes the turbine in parked condition with a mean wind speed of 44 m/s and with extreme sea state. ~~The simulations~~ This load case consists of 18 ~~realizations (i.e. six~~ simulations (1 wind speed $\times$ 3 wave periods $\times$ 6 seeds). In Figure 8 the nacelle acceleration, tower-base bending moment and planar motions of the floater are shown. Furthermore Table 9 shows the deviation values of the two models.

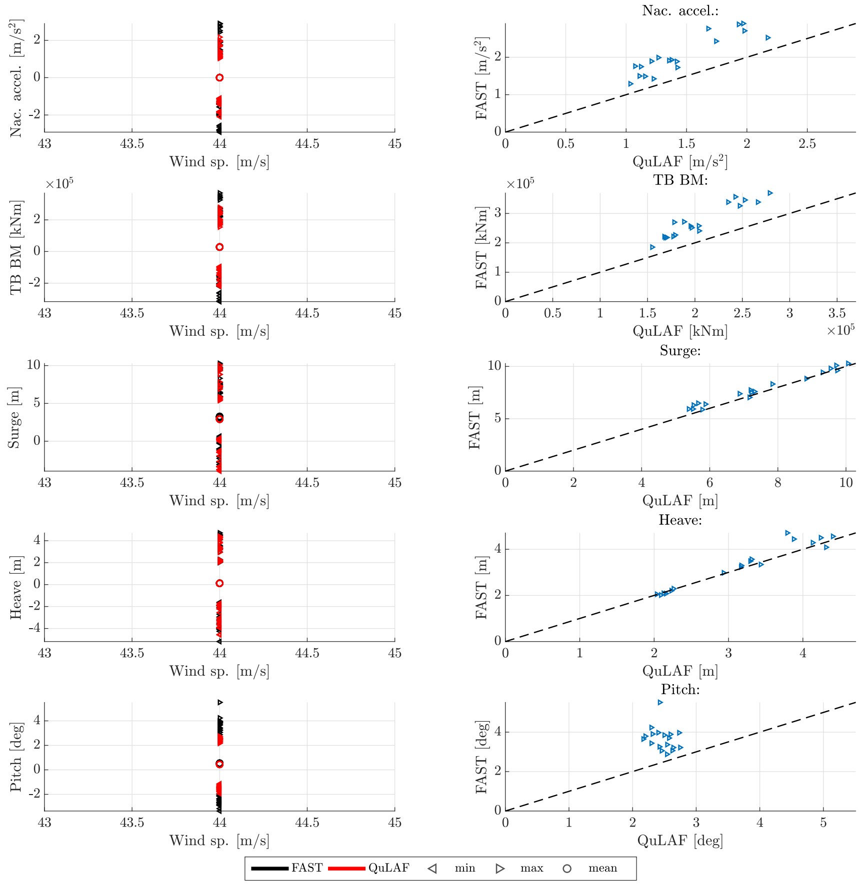

Figure 8. Response to DLC6.1 for FAST and QuLAF. Left: min., max. and mean values for every realisation as function of wind speed. Right: maximum values for FAST as function of the corresponding maximum values in QuLAF

Overall the results are similar to DLC 1.6 at 5 m/s, since the thrust level is nearly the same for that case and both load cases utilises the extreme sea state. The nacelle acceleration, tower-base bending moment and pitch motion all show an under-prediction by QuLAF which can be explained by limitation of A, regarding the missing viscous effects. Surge and heave, on the other hand, are ~~matched very well~~ well matched with a deviation of 5% and 3% respectively.

Table 9. Mean values Ratio of the response ratios of the max. values response (QuLAF/FAST) averaged per wind speed for DLC6.1.

Mean(X_{Qulaf}/X_{FAST} $X_{Qulaf,max}/X_{FAST,max}$) [−]	Wind speed [m/s] 44.0
Nac. Accel.	0.72
TB BM	0.76
Surge	0.95
Heave	0.97
Pitch	0.69

5.4 Summary of ULS study

To summarize the ULS study, an overview of the ultimate load and response populations are presented in a boxplot for each of the five load cases in Figure 9. This way the critical cases can be identified and compared for the two models. The boxplots show the minimum, first quantile, median (line in the center of the box), third quantile and the maximum of the data for each wind speed. The ultimate load and response values in the summary plot are obtained as a mean of all the maximum values for each seed associated with the specific environmental condition.

It can be seen that the ultimate nacelle accelerations are governed by the extreme sea state, thus DLC 1.6 and DLC 6.1. Both models agree on this conclusion but with an under-prediction of the values in QuLAF, due to limitation A. The ultimate tower-base bending moments and pitch motion are obtained in DLC 1.6 and DLC 1.3, respectively and both models agree very well on the values. Similarly the largest heave motions are generally very well matched by QuLAF, since it is always dominated by waves and the hydrostatics are modelled the same way in both models, hence the largest response is obtained in the extreme sea states. The largest surge motions are obtained in DLC1.3 with an over-prediction of the response in QuLAF, likely due to limitation B and C, but with an slight under-prediction in all other load cases.

In order to investigate whether the models predict the same design-driving cases, the ranking of the eight highest maximum values of the nacelle acceleration, tower-base bending moment and planar motions with their corresponding load case simulation are presented in Figure 10.

The load levels are generally in good agreement. Looking at the nacelle acceleration, the values are under-predicted by QuLAF but the two models agree on the same governing load cases. For the tower-base bending moment, the two models agree very well show a agreement in both maximum values (up to %6 deviation) and load cases, where the maximum tower bending moments for both models are obtained in severe sea states around rated wind speed. Generally both models predict that the highest surge and pitch motions are obtained in extreme turbulence just below rated wind speed, but with a slight over-prediction in QuLAF.

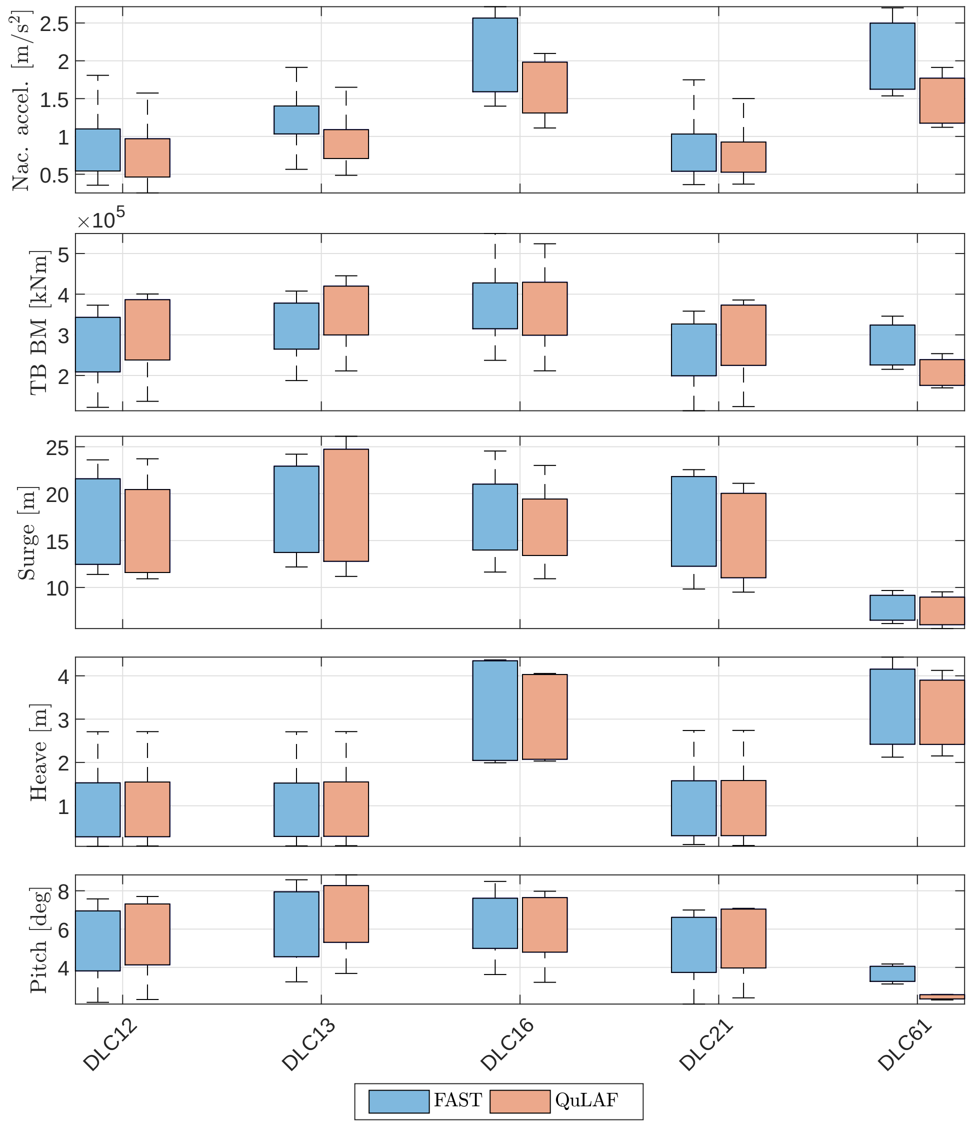

Figure 9. Population of max. values for each of the five load cases

All load cases have shown a good agreement in heave (up to %8 deviation), which is due to the fact that it is dominated by hydrodynamic forcing. Both wave loads, hydrostatics and hydrodynamic inertia loads are modelled the same way in the two models. Differences exist mainly in the viscous loads and mooring stiffness, but the effect of these on heave is less important.

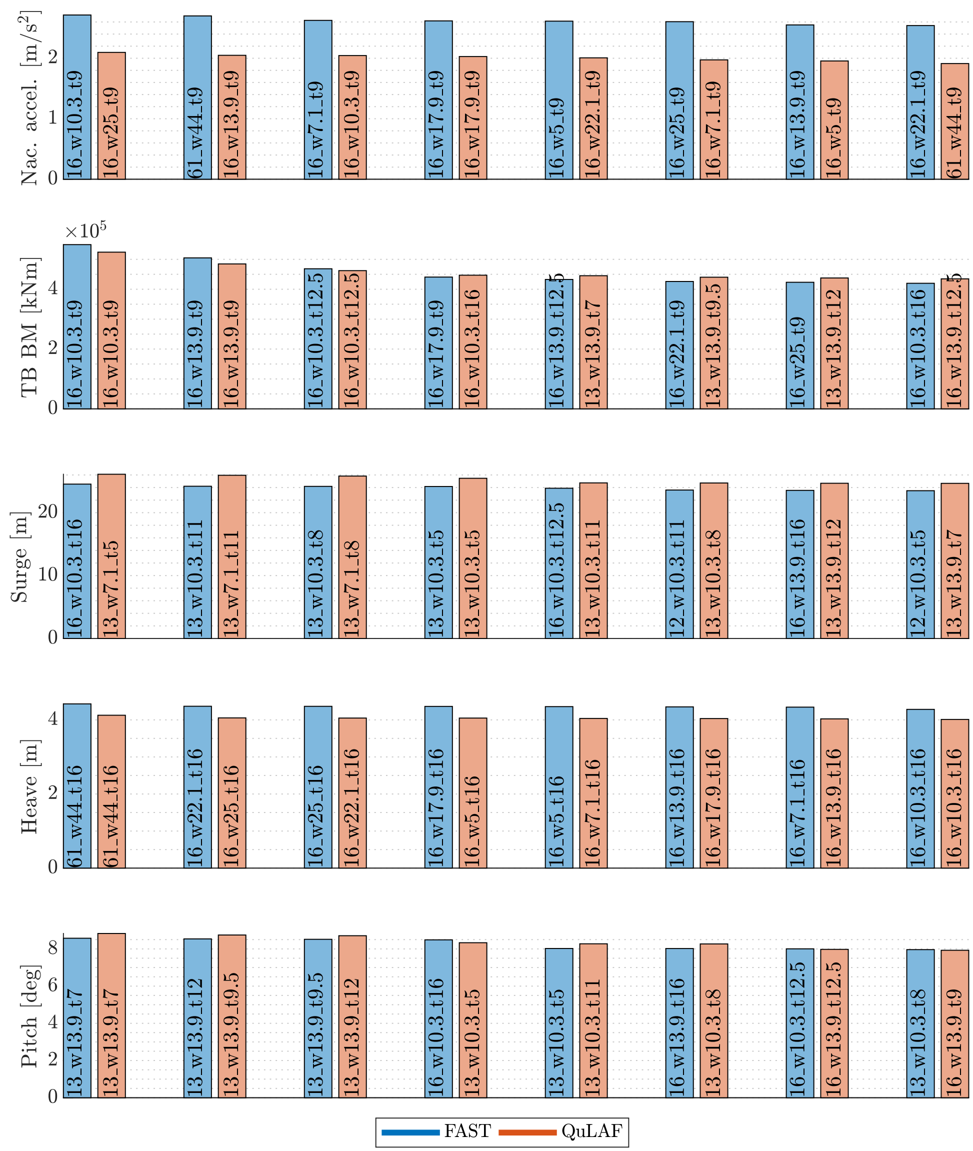

Figure 10. Ranking of the eight highest max. values of each signal and corresponding load case simulations for FAST and QuLAF. The text in each box follows the pattern of design load case, mean wind speed and then wave period, i.e. *dlc_wsp_tp*.

6 Limitation study

Following the main results from the study, the limitations of the QuLAF model (Section 3.3) are now investigated further with the purpose to asses their impact on the response.

6.1 Omission of viscous drag forcing

First we look at limitation A, where the results for the severe sea state of DLC1.6 (Figure 5) are repeated, but with the viscous drag loads disabled in both models. Since the waves are dominating, both models should give very similar response for this case. For this comparison only, an additional constant linear damping matrix was included in both models to avoid unphysical resonant responses, mostly in QuLAF for the heave DoF. When disabling the viscous effects in QuLAF, the only damping contribution left in the heave DoF is the radiation damping, which is very low at the heave natural frequency and is therefore not sufficient to avoid unphysical resonant response in heave. In FAST, on the other hand, the dynamic representation of the mooring system introduces both viscous damping and nonlinear stiffness that limit the resonant response in heave. Figure 11 shows the results. A ~~very close~~ good match in the nacelle acceleration, tower-base bending moment and all floater motions is now seen. By comparison to Figure 5 (DLC1.6 with viscous effects in FAST) we clearly see the effect of the omission of viscous drag forcing in QuLAF.

Limitation A is thus confirmed and can explain the under-prediction of the nacelle acceleration, tower-base bending moment and floater motions in QuLAF for the load cases where the waves are dominating, i.e. DLC1.6 and DLC6.1.

6.2 Simplified rotor-induced forcing and damping

Secondly we investigate the complexity of extracting aerodynamic loads around rated wind speed, where the controller switches between the partial- and full-load regions, i.e. limitation B. A study was made comparing the extracted aerodynamic forcing for surge, pitch and tower deflection in the full FAST model setup and the response-locked loads plus damping setup, which is utilized in QuLAF.

We extract the aerodynamic rotor loads from the full FAST computation, and compare them to the aerodynamic rotor loads applied in QuLAF. This is done with basis in the shaft loads from FAST, which are next subtracted inertial and gravitational effects. Based on a free body diagram (see Figure 12) the purely aerodynamic rotor loads in the full FAST computation are calculated as

$$F_{Ax,full} = F_{Sx} + M_{rh}\,\ddot{x}_{hub}, \tag{2}$$

$$\tau_{A,full} = \tau_S + M_{rh}\,g\,|BA|\cos\theta_{hub} + I_{rh}\,\ddot{\theta}_{hub} + M_{rh}\,\ddot{x}_{hub}\,|BA|\sin\theta_{hub} + M_{rh}\,\ddot{z}_{hub}\,|BA|\cos\theta_{hub}. \tag{3}$$

Here A is the point of output for the shaft loads in FAST, B is the position of the rotor centre of gravity and $|BA|$ is the distance from A to B. The shaft force F_S is defined in its own coordinate system and consists of a normal and tangential shaft force. Hence the global x-component is determined from vector transformation. The angle θ_{hub} is the sum of the fixed tilt angle and

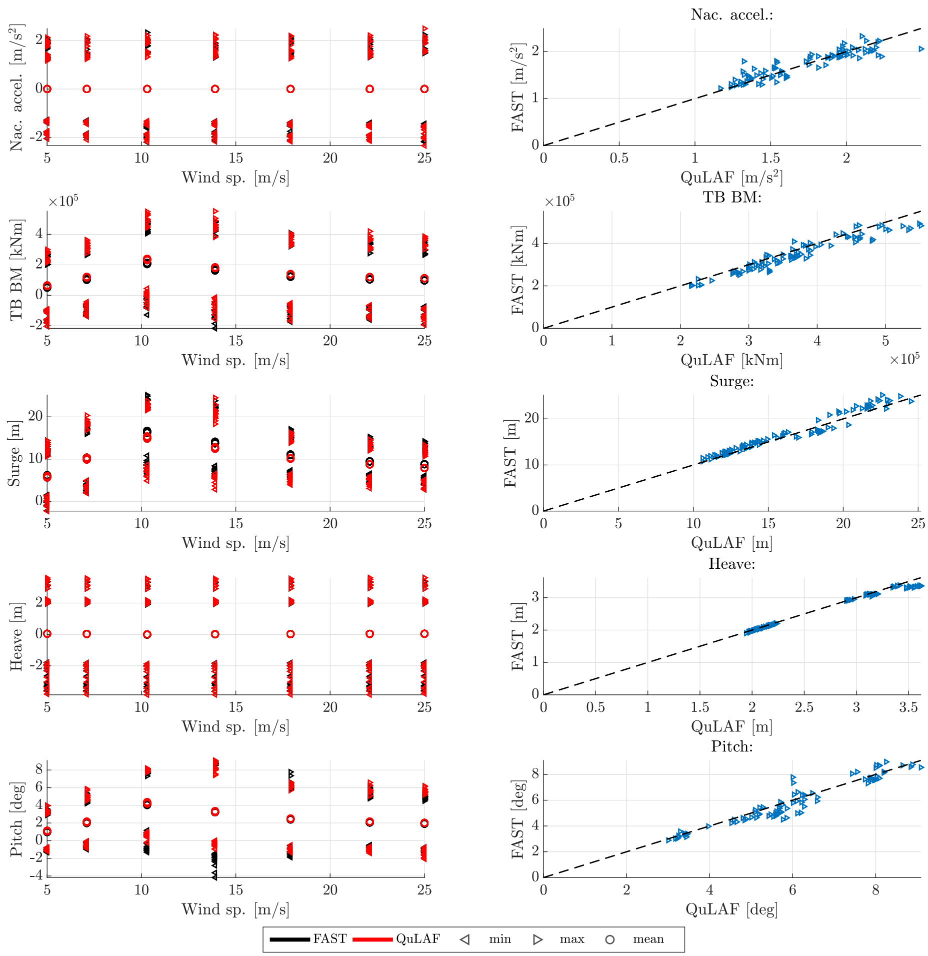

Figure 11. Response to DLC1.6 (**without** viscous drag) for FAST and QuLAF. Left: min., max. and mean values for every realisation as function of wind speed. Right: maximum values for FAST as function of the corresponding maximum values in QuLAF

the instantaneous hub deflection angle. The rotor and hub mass and the mass moment of inertia around point A are denoted M_{rh} and I_{rh} respectively. Lastly x_{hub} and z_{hub} are the horizontal and vertical translation of the hub centre of gravity.

The same equations with $\ddot{x}_{hub}$, $\ddot{z}_{hub}$, $\ddot{\theta}_{hub} = 0$ ~~where~~ were applied in the original response-locked FAST calculations for the extraction of the loads for QuLAF. We will refer to the latter as the simplified method.

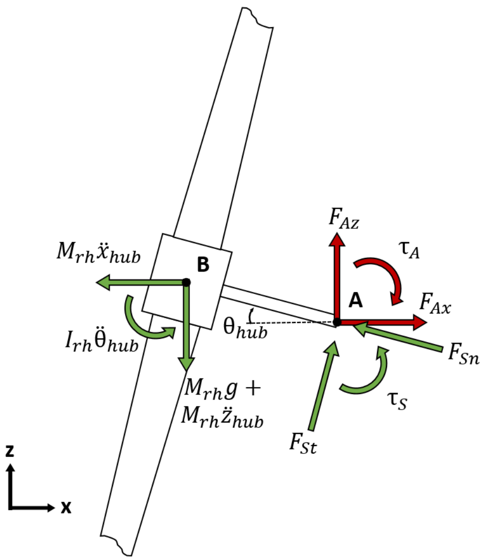

Figure 12. Free body diagram of the rotor

In QuLAF the extracted forcing (for a response-locked nacelle) and damping are applied in the surge, pitch and tower deflection degrees of freedom as described in Pegalajar-Jurado et al. (2018a):

$$F_{surge,simple} = F_{Ax,simple} - B_{11}\,\dot{\xi}_1, \tag{4}$$

$$F_{pitch,simple} = F_{Ax,simple}\,h_{hub} + \tau_{A,simple} - B_{55}\,\dot{\xi}_5, \tag{5}$$

$$F_{tower,simple} = F_{Ax,simple}\,\phi_{hub} + \tau_{A,simple}\,\frac{\partial \phi_{hub}}{\partial z} - B_{tower}\,\dot{\alpha}. \tag{6}$$

Here h_{hub} is the hub height, the mode shape deflection evaluated at the hub is ϕ_{hub} and B_{11}, B_{55} and B_{tower} are the aerodynamic damping terms for surge ξ_1, pitch ξ_5 and tower deflection α degrees of freedom respectively.

The loads are applied in the undeflected point B, which is consistent with the linearisation and with further neglection of the $F_{St}|BA|$ moment correction from A to B.

We now compare these to the similar forcing based on the extracted loads from the full FAST computations, which include damping implicitly:

$$F_{surge,full} = F_{Ax,full} \tag{7}$$

$$F_{pitch,full} = F_{Ax,full}\,h_{hub} + \tau_{A,full} \tag{8}$$

$$F_{tower,full} = F_{Ax,full}\,\phi_{hub} + \tau_{A,full}\,\frac{\partial \phi_{hub}}{\partial z} \tag{9}$$

The combined comparison of both forcing and damping in the simplified approach is needed since the damping cannot be extracted as an isolated component from the full FAST computations. To focus on the loads, the full FAST response results for $\dot{\xi}_1$, $\dot{\xi}_5$ and $\dot{\delta}$ were applied in the calculation of the damping contribution in F_{simple}.

Figure 13 and 14 show the extracted aerodynamic forcing applied in the surge, pitch and tower deflection degrees of freedom together with the rotor speed and blade pitch angle for the case of extreme turbulence (DLC1.3). The two cases are conducted for a wind speed of $10.3\,\mathrm{m/s}$ and $13.9\,\mathrm{m/s}$, hence just below and above rated wind speed in order to asses the effect of the switching between the control regions.

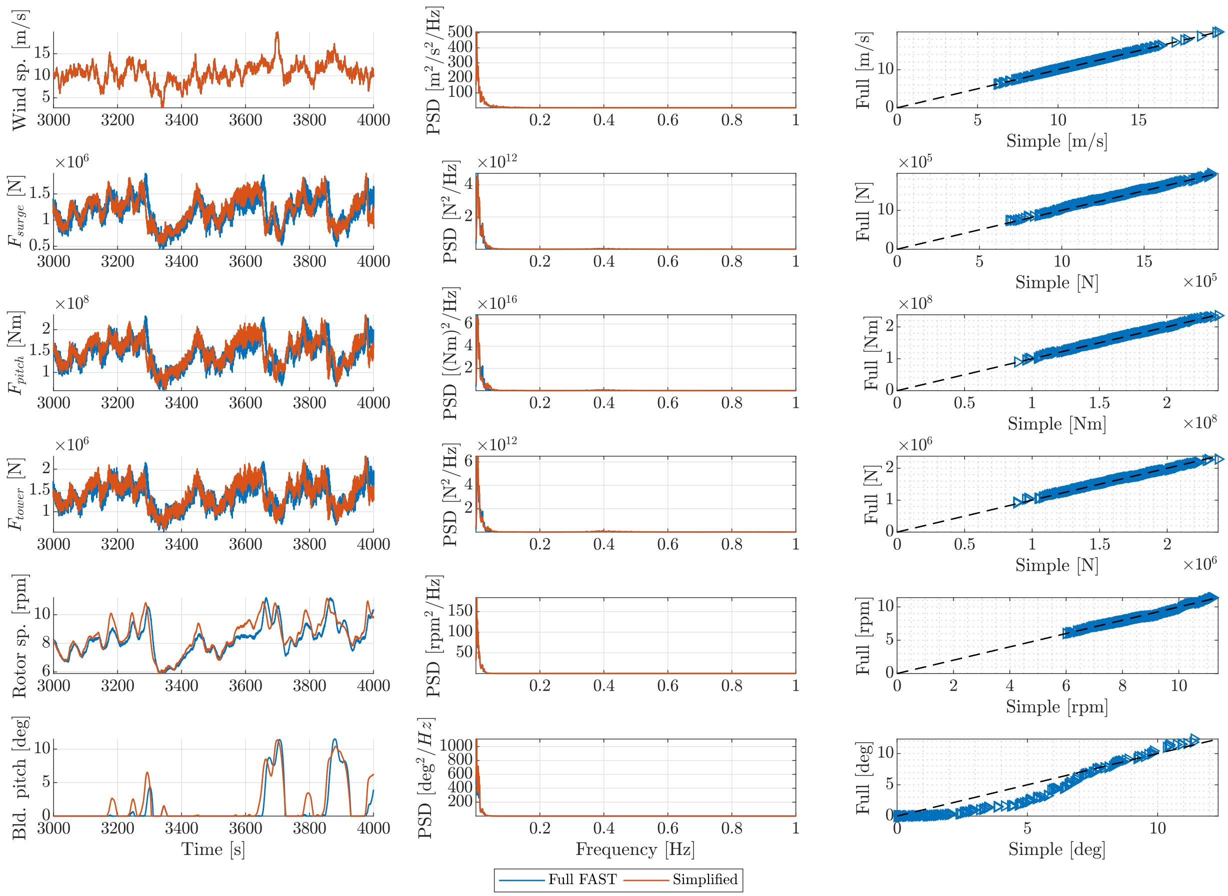

Figure 13. Extracted aerodynamic forcing applied in the surge, pitch and tower deflection degrees of freedom and turbine operational data for DLC1.3 with $10.3\,\mathrm{m/s}$ mean wind speed. Left: time series outline. Middle: corresponding power density spectrum (PDF). Right: peak values (sorted) for the full FAST computations as function of the corresponding maximum values in the simplified method.

It is observed that the applied aerodynamic forcing in the surge, pitch and tower deflection degrees of freedom below rated wind speed are matched ~~very~~ well. From the blade pitch angle in Figure 13, it can be seen that the response-locked computations switches significantly more between the control regions compared to the full FAST computations. This is to be expected as the fixed nacelle configuration will feel larger peaks of the wind speed compared to the full FAST computations. Then looking at the full FAST computations, a slight over-prediction of the aerodynamic forcing term in surge, pitch and tower is seen, but the maximum values match well with the full FAST computations.

Limitation B is thus found to have a minor impact on the results. Apart from a small under-prediction at $13.9\,\mathrm{m/s}$ mean wind speed, the wind-induced loads are matched remarkable well by QuLAF.

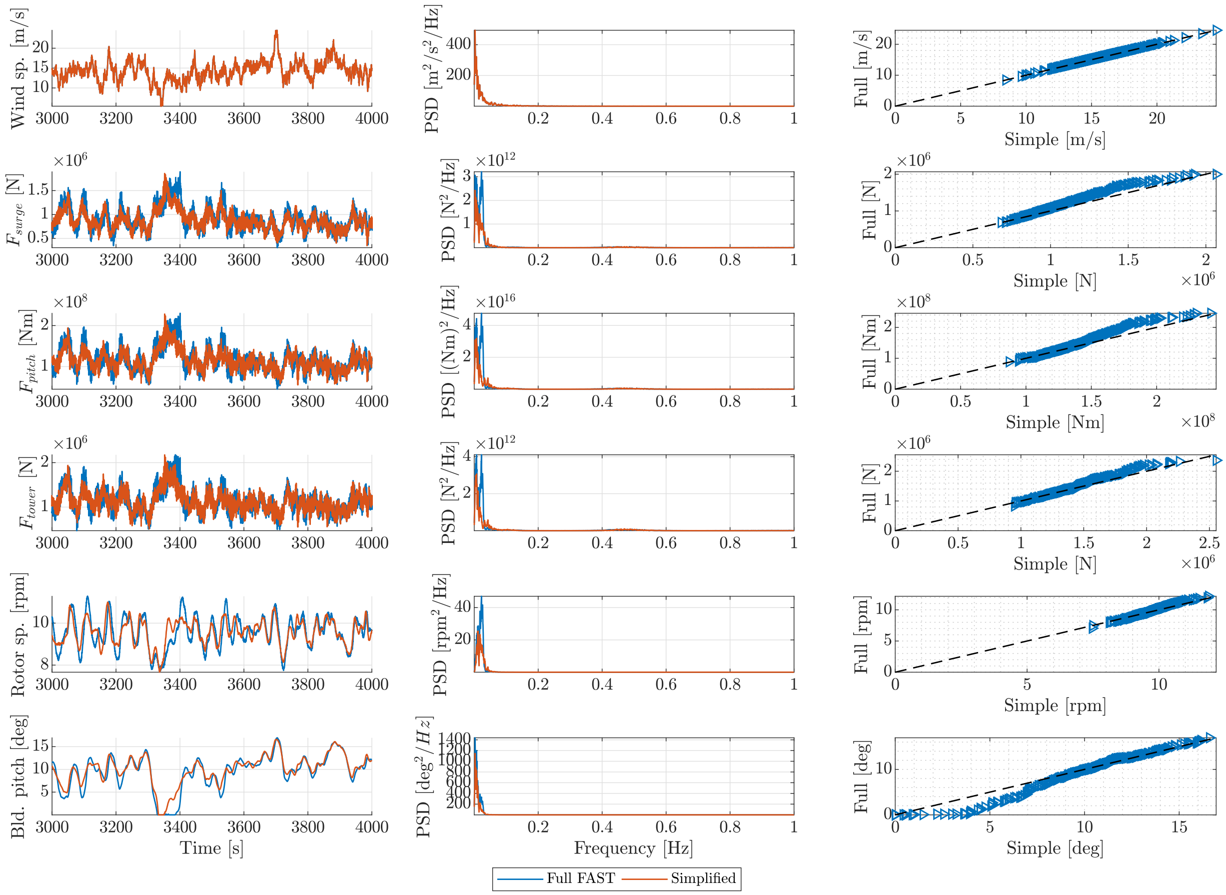

Figure 14. Extracted aerodynamic forcing applied in the surge, pitch and tower deflection degrees of freedom and turbine operational data for DLC1.3 with $13.9\,\mathrm{m/s}$ mean wind speed. Left: time series outline. Middle: corresponding power density spectrum (PDF). Right: peak values (sorted) for the full FAST computations as function of the corresponding maximum values in the simplified method.

6.3 Over-predicted tower damping

Finally limitation C, regarding the extraction of aerodynamic damping, is investigated. Figure 15 shows the aerodynamic damping ratio as function of the natural frequency of the tower. It is observed that the aerodynamic damping decreases with tower frequency. Since the aerodynamic damping in QuLAF is extracted for a clamped tower with rigid blades, i.e. at a lower natural frequency compared to the full FAST model, the aerodynamic damping for the tower mode motion will be over-predicted, leading to a under-prediction of the tower response and nacelle acceleration in QuLAF. Also the under-predicted tower frequency in QuLAF relative to FAST (0.682 Hz vs 0.746 Hz) will lead to smaller accelerations for the same motion amplitude.

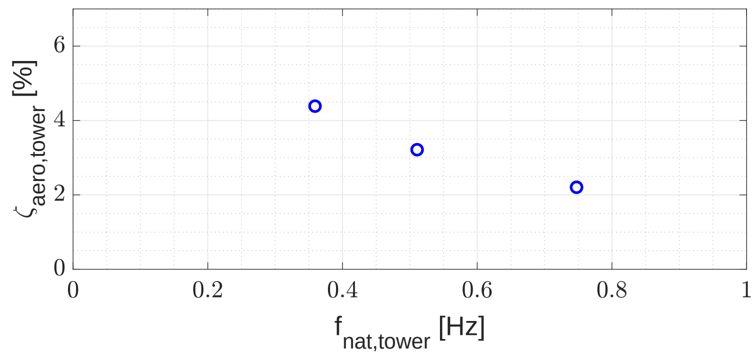

Figure 15. Dependency of aerodynamic damping on tower natural frequency for $W = 15\,\mathrm{m/s}$.

Limitation C is thus confirmed and can explain the large under-prediction of the nacelle acceleration in the FLS study and in DLC1.2 and DLC1.3 of the ULS study.

7 Conclusions

Based on a selected subset of critical load cases, the accuracy of the simplified model QuLAF for different load cases has been investigated through comparison to a FAST state-of-the-art model. The study was based on the OO-Star Wind Floater Semi 10MW floater and the DTU 10MW reference wind turbine. The model accuracy was assessed both in terms of an FLS analysis and a ULS analysis.

The FLS analysis showed that the simplified model was very good at estimating the damage-equivalent bending moment at the tower base, but it systematically under-predicted the nacelle acceleration. The high under-prediction in the nacelle acceleration is likely due to the tower vibrations being too damped. The same picture of the nacelle acceleration being under-predicted in the simplified model was also present in the ULS analysis. The largest tower-base bending moments were generally over-predicted, but it was observed that stronger wind would lead to an over-prediction whereas stronger waves would lead to an under-prediction. However, the largest load was obtained at 10.3 m/s in DLC 1.6 and here the effects compensated each other and gave a ~~perfect~~ good match between the two models. Regarding the platform motions, the largest surge responses were observed in DLC 1.3 and DLC 1.6 with a 3% over-prediction and 11% under-prediction, respectively. The largest heave motions were generally ~~very~~ well matched by the two models and presented highest values in the ESS cases. ~~Lastly~~Further, the ultimate pitch responses were obtained in DLC 1.3 and DLC 1.6 (both at rated conditions) and within 4% deviation. Lastly, for the emergency stop case of DLC 2.1, comparisons at the time series level showed that QuLAF is able to reproduce a transient event.

Analysis of the model limitations confirmed that the omission of viscous hydrodynamic loads is the cause of under-estimated response for large sea states. Also the over-estimated damping of the tower mode was confirmed and explained by the frequency dependency of the damping, which implies a larger damping level for the clamped tower configuration. Re-calibration of this damping is straight-forward but will be configuration specific. Finally, a close inspection of the rotor-induced loads showed that the decoupled approach of QuLAF with linear damping provides very accurate loads when compared to a full FAST simulation. Based on the results at two wind speeds, there seem to be no strong limitation in this simple approach to rotor loads, even for a configuration with multiple degrees of freedom.

Despite its limitations, QuLAF has been found to be a quite accurate load and response prediction tool for the five aligned wind-wave load cases (DLC 1.2, 1.3, 1.6, 2.1 and 6.1), especially for tower-base bending moments, heave and pitch motions. The model can therefore be used as a tool to explore the design space in the preliminary design stages of a floating platform for offshore wind. The model can quickly give an estimate of the main natural frequencies, response and loads for a wide range of environmental conditions, which makes it useful for optimization loops. A full aero-hydro-servo-elastic model is still necessary to assess the performance in a wider range of environmental conditions, including non-linearities, fault conditions and real-time control.

Acknowledgements

This work is part of the LIFES50+ project (http://lifes50plus.eu) and the research leading to these results has received funding from the European Union's Horizon 2020 research and innovation programme under grant agreement No. 640741. Discussions with Frank Lemmer, Kolja Müller, Yu Wei (University of Stuttgart), Denis Martha (Rambøll) and Andreas Manjock (DNV-GL) are gratefully acknowledged.

References

61400-3, I.: Wind turbines - Part 3: Design Requirements for Offshore Wind Turbines, https://webstore.iec.ch/publication/5446, 2009.

Bak, C., Zahle, F., Bitsche, R., Kim, T., Yde, A., Henriksen, L., Natarajan, A., and Hansen, M.: Description of the DTU 10 MW reference wind turbine, Tech. rep., No. I-0092, DTU Wind Energy, 2013.

Hansen, M. and Henriksen, L.: Basic DTU Wind Energy controller, Tech. rep., No. E-0028, DTU Wind Energy, 2013.

Hansen, M., Hansen, A., Larsen, T., Øye, S., Sørensen, P., and Fuglsang, P.: Control design for a pitch-regulated, variable-speed wind turbine, Tech. rep., No. Risø-R-1500(EN), Risø National Laboratory, 2005.

Jonkman, J. and Jonkman, B.: NWTC Information Portal (FAST v8), https://nwtc.nrel.gov/FAST8, 2016.

Krieger, A., Ramachandran, G., Vita, L., Gómez-Alonso, G., Berque, J., and Aguirre, G.: LIFES50+ D7.2: Design basis, Tech. rep., DNV-GL, 2015.

Lee, C. and Newman, J.: WAMIT, http://www.wamit.com/, 2016.

Lemmer, F., Müller, K., Pegalajar-Jurado, A., Borg, M., and Bredmose, H.: LIFES50+ D4.1: Simple numerical models for upscaled design, Tech. rep., University of Stuttgart, 2016.

Müller, K., Faerron-Guzman, R., Borg, M., and Manjock, A.: LIFES50+ D7.7: Identification of critical environmental conditions and design load cases, Tech. rep., University of Stuttgart, 2018.

Pegalajar-Jurado, A., Borg, M., and Bredmose, H.: An efficient frequency-domain model for quick load analysis of floating offshore wind turbines, Wind Energy Science, 3, 693–712, https://doi.org/10.5194/wes-3-693-2018, 2018a.

Pegalajar-Jurado, A., Bredmose, H., Borg, M., Straume, J., Landbø, T., Andersen, H., Yu, W., Müller, K., and Lemmer, F.: State-of-the-art model for the LIFES50+ OO-Star Wind Floater Semi 10MW floating wind turbine, Journal of Physics: Conference Series, 1104, 012 024, https://doi.org/10.1088/1742-6596/1104/1/012024, 2018b.

Pegalajar-Jurado, A., Madsen, F., Borg, M., and Bredmose, H.: LIFES50+ D4.5: State-of-the-art models for the two LIFES50+ 10MW floater concepts, Tech. rep., Technical University of Denmark, 2018c.

Schafhirt, S. and Muskulus, M.: Decoupled simulations of offshore wind turbines with reduced rotor loads and aerodynamic damping, Wind Energy Science, 3, 25–41, https://doi.org/10.5194/wes-3-25-2018, 2018.

Schløer, S., Garcia-Castillo, L., Fejerskov, M., Stroescu, E., and Bredmose, H.: A model for Quick Load Analysis for monopile-type offshore wind turbine substructures, Journal of Physics: Conference Series, 753, 092 008, https://doi.org/10.1088/1742-6596/753/9/092008, 2016.

Schløer, S., Garcia-Castillo, L., Fejerskov, M., Stroescu, E., and Bredmose, H.: A model for quick load analysis for monopile-type offshore wind turbine substructures, Wind Energy Science, 3, 57–73, https://doi.org/10.5194/wes-2017-11, 2018.

Yu, W., Müller, K., and Lemmer, F.: LIFES50+ D4.2: Public definition of the two LIFES50+ 10MW floater concepts, Tech. rep., University of Stuttgart, 2018.